ACS Catalysis

pubs.acs.org/acscatalysis
Research Article

Directed Evolution of Material Binding Peptide for Polylactic Acid-specific Degradation in Mixed Plastic Wastes

Yi Lu, Kai-Wolfgang Hintzen, Tetiana Kurkina, Yu Ji,* and Ulrich Schwaneberg*

Cite This: ACS Catal. 2023, 13, 12746−12754
Read Online

ACCESS | Metrics & More | Article Recommendations | Supporting Information

ABSTRACT: In order to preserve our livelihood for future generations, responsible use of plastics in a climate-neutral and circular economy has to be developed so that plastics can be used in an environmentally friendly way by future generations. The prerequisite is that bioplastic polymers such as polylactic acid (PLA) can be efficiently recycled from petrochemical based plastic. Here, a concept in which accelerated PLA degradation in the mixed suspension of PLA and polystyrene (PS) nanoparticles has been achieved through an engineered material binding peptide. After comparison of twenty material binding peptides, Cg-Def is selected due to its PLA binding specificity. Finally, a suitable high-throughput screening system is developed for enhancing material-specific binding toward PLA in presence of PS. Through KnowVolution campaign, a variant Cg-Def YH (L9Y/S19H) with 2.0-fold improved PLA binding specificity compared to PS is generated. Contact angle and surface plasmon resonance measurements validated higher surface coverage of Cg-Def YH on PLA surface and the fusion of Cg-Def YH with PLA degrading enzyme confirmed the accelerated PLA depolymerization (two times higher than only enzyme) in mixed PLA/PS plastics.

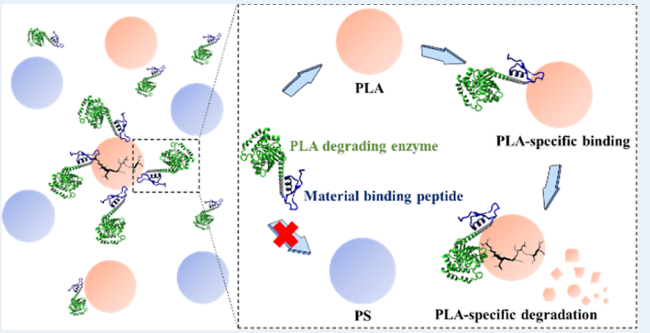

KEYWORDS: *directed evolution, plastic degradation, polylactic acid, material binding peptide, circular economy*

1. INTRODUCTION

Plastic products are extensively used in our daily lives due to their excellent properties and are produced in large quantities (>390 million tonnes in 2021).[1,2] Management of plastic waste is an important challenge to mitigate risks to living organisms and humans.[3−6] Commonly used plastics comprise polyethylene (PE), polypropylene (PP), polystyrene (PS), poly(ethylene terephthalate) (PET), and polyurethane (PU), which are mostly produced from fossil fuels.[7] In order to address risks caused by climate change, researchers have proposed to replace conventional petrochemical-based plastics with bioplastics made from feedstock and to implement strategies for circular use as a foundation for a climate-neutral circular economy.[8,9] Polylactic acid (PLA), a polyester produced from renewable sources such as starch or sugar, is from its performance an attractive and biocompatible polymer.[10] PLA is often blended with other petrochemical polymers like poly(ε-caprolactone) (PCL), polybutylene succinate (PBS), thermoplastic starch (TPS), PE, PP, and PS, to optimize hydrophobicity, mechanical behavior, and reduce production costs.[11−13] Among them, PS is one of the most hydrophobic plastics.[14,15] PLA/PS blends are used in diverse applications such as drug delivery,[16] electronic equipment,[17] and packaging.[18] For instance, Li et al.[19] reported that the PLA/PS (50/50 wt %) blend composite exhibited a significantly higher conductivity and is used in devices to detect volatile organic compounds. Therefore, exploring efficient recycling methods for mixed plastics of PLA/PS is of high interest.[20−23] For PLA enzymatic degradation, many enzymes such as proteinase K, esterases, lipases, and cutinases have been discovered.[24] They are classified as type I (proteases) and type II (cutinases/esterases/lipases) PLA degrading enzymes.[25] Interestingly, two PET degrading enzymes, Thc_Cut1 and Thc_Cut2 from *Thermobifida cellulosilytica*, were used in PLA degradation.[26] This indicates that PET depolymerases have huge potential in PLA degradation. To the best of our knowledge, no enzymatic degradation of PLA in mixed plastics has been reported.

Material binding peptides (MBPs), also referred to as anchor peptides or adhesion promoting peptides, have been identified for a variety of natural and manmade materials such as synthetic polymers (e.g., PP,[27] PS,[28] and PUR[29]), metals (e.g., stainless steel[30,31] and gold[31]), silicon wafer,[31] and plant leaves.[32−35] The binding property of MBPs, such as binding strength or material binding specificity, can be tailored by

Received: May 11, 2023
Revised: August 8, 2023
Published: September 15, 2023

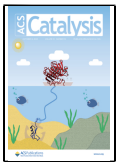

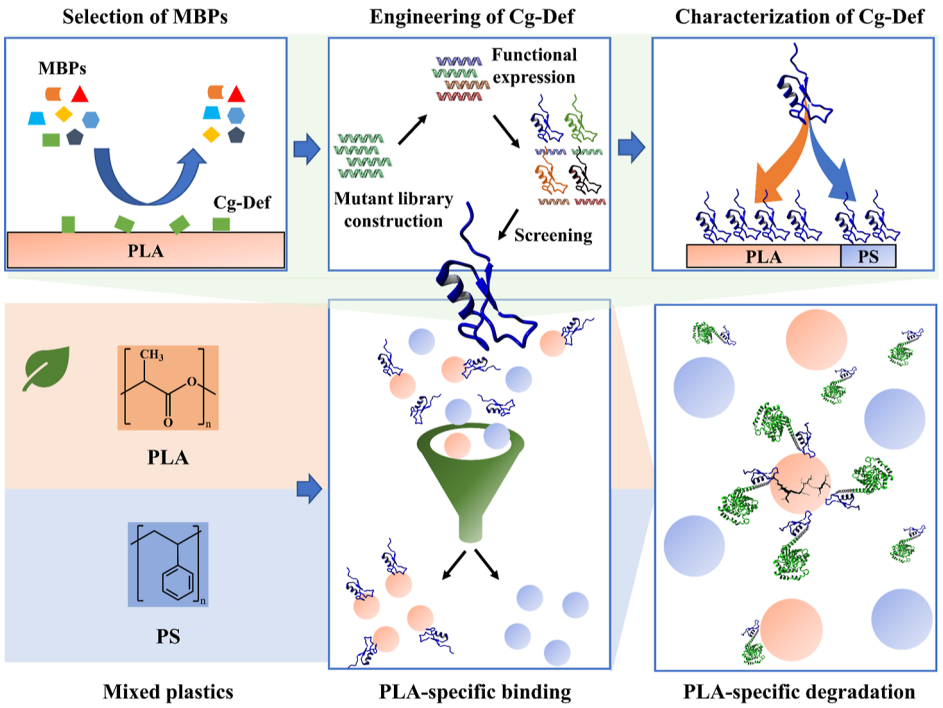

Figure 1. Specific degradation of bio-based plastic PLA in mixed plastic wastes with the assistance of MBPs. The engineered Cg-Def variants by KnowVolution strategy could endow the PLA degrading enzyme with high PLA binding specificity from PS and, therefore, accelerating PLA degradation in the PLA/PS mixed plastic wastes. PLA: polylactic acid; MBP: material binding peptides; PS: polystyrene.

protein engineering methodologies following for instance the KnowVolution (knowledge-gaining directed evolution) strategy, which combines four phases of experimental work and computational design to minimize experimental work and maximize property improvements.[36] KnowVolution is a generally applicable approach to improve various properties of proteins including activity,[37] thermal resistance,[38] pH resistance,[39] regioselectivity,[40] ionic liquid resistance,[41] and polymer processivity.[42] In addition, KnowVolution has successfully been applied to tailor the material binding properties of MBPs.[27]

MBPs such as polymer binding modules, anchor peptides, carbohydrate binding modules (CBMs), hydrophobins, chitin binding domain, and hydrophobic binding domain, have been widely applied to accelerate the enzymatic degradation of natural polymers (e.g., cellulose, lignin, and chitin) and synthetic polymers [e.g., PU, poly-β-hydroxybutyrate (PHB), and PET].[43−45] In natural polymers degradation, CBMs potentiate the activity of catalytic domain of cellulase against cellulose by directing cellulase toward cellulose and thereby tuning the affinity of cellulase into the most productive range.[44] Inspired by nature, a lot of research has been conducted to facilitate PET enzymatic degradation by fusing engineered MBPs with single PET hydrolase or enzyme complex.[46−48] The first report to use a MBP for man-made polymer degradation was reported by Islam et al.,[49] which cleaved the ester bonds in polyester−polyurethane nanoparticles. Likely inspired by this work, further MBPs have been used to bind to PET by hydrophobic interaction and hydrogen bond.[50] For instance, Xue et al.[48] fused a chitin-binding domain (ChBD) with PET hydrolase ICCG. Compared with ICCG alone, ICCG-ChBD displayed higher PET adsorption and improved degradation performance (19.6% higher than ICCG). Moreover, Chen et al.[51] codisplayed PETase and hydrophobin HFBI on the surface of yeast cells. The turnover rate of the whole-cell biocatalyst toward high-crystallinity PET (45%) dramatically increases approximately 328.8-fold compared with that of purified PETase at 30 °C. However, the improvement in the polymer degradation by MBPs can be significantly influenced by the concentration of polymers. Graham et al.[46] found that CBMs could accelerate PET enzymatic degradation at low PET loading (<10 wt %) and the enhanced degradation cannot be observed at high PET loading (10−20 wt %). The limited activity of polymer hydrolase-MBP fusion at higher substrate concentration would hinder the industrial application of MBPs in plastic enzymatic recycling.

In this work, MBP Cg-Def was selected from several MBPs and engineered following the KnowVolution strategy to achieve an enhanced material-specific binding of PLA in mixed PLA/PS. To the best of our knowledge, no reported MBP has been improved in its material-specific binding properties to enhance the depolymerization of mixed plastics. A prerequisite for any successful protein engineering campaign is robust and sensitive high throughput screening systems [e.g., 96-well microtiter plate (MTP) format] that reflect application conditions. The KnowVolution campaign yielded a Cg-Def variant with enhanced PLA binding specificity in PLA/PS mixtures. A depolymerase ICCG[52] was identified with outstanding performance in PLA degradation within this study. Fusion of the engineered Cg-Def variant with ICCG resulted in enhanced PLA degradation in mixed PLA/PS.

2. RESULTS AND DISCUSSION

Material-specific degradation in mixed plastics is important for the circular polymer economy. In Figure 1, the typical procedures are summarized to enhance PLA degradation in mixed PLA/PS plastic as a first step toward a circular PLA economy. Three MBPs with different sizes, secondary

https://doi.org/10.1021/acscatal.3c02142
ACS Catal. 2023, 13, 12746−12754

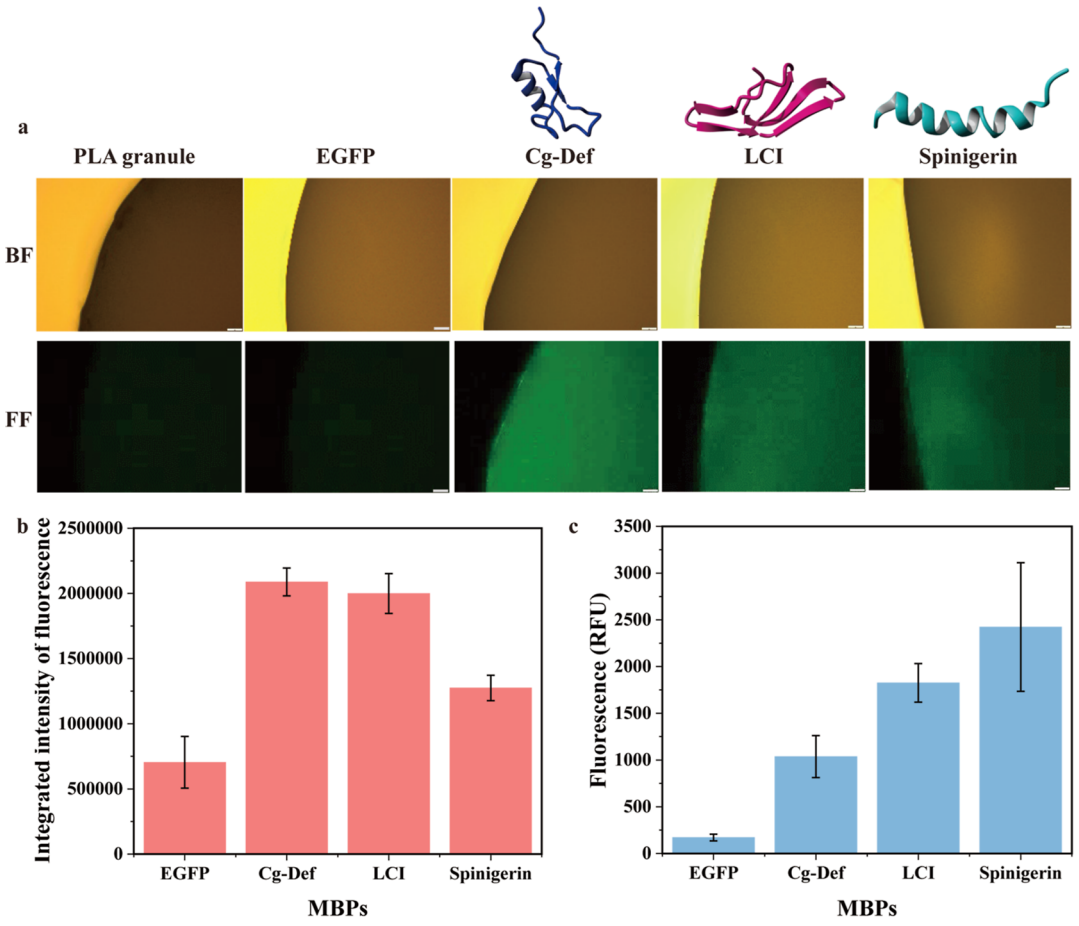

Figure 2. MBP selection with potential PLA binding specificity from PS. (a) Fluorescence microscopy images of bare PLA granules and PLA granules bound with EGFP (negative control), Cg-Def, LCI, and Spinigerin. Fluorescence microscopy was taken at exc. 485 nm and em. 520 nm. The scale bar represented 20 μm. (b) Comparison of PLA binding performance of three MBPs including EGFP, Cg-Def, LCI, and Spinigerin. PLA binding of three MBPs was indicated by integrated intensity of fluorescence, which was measured based on fluorescence microscopy pictures of MBPs bound to PLA granules with ImageJ software.[56] The experiments were performed in triplicate. (c) Comparison of PS binding performance of three MBPs including EGFP, Cg-Def, LCI, and Spinigerin. The experiments were performed in triplicate. Concentration of MBPs used for binding was 2.5 μM. The PLA granules and PS MTPs were washed with Tris−HCl twice and LAS once after binding with MBPs at room temperature for 10 min. PLA: polylactic acid; MBP: material binding peptides; PS: polystyrene; BF: bright field, FF: fluorescence field; LAS: alkyl benzene sulfonate.

structures, and properties were expressed, purified, and probed with respect to their PLA binding strength and specificity, which resulted in the selection of Cg-Def as a good starting point for the protein engineering study. Improved PLA-specific binding of a Cg-Def variant was achieved in a single KnowVolution campaign and enhanced material-specific binding was confirmed through biophysical characterizations including contact angle and surface plasmon resonance (SPR) measurement. PLA-targeted depolymerization in mixed PLA/PS was determined as final proof of Cg-Def enhanced degradation of PLA in a PLA/PS mixture.

2.1. Selection of MBP with Potential PLA Binding Specificity from PS. Three MBPs including Cg-Def, LCI, and Spinigerin exceeded other MBPs (higher fluorescence intensity) when the binding of 20 MBPs to PLA granules was compared (Figure S2 and Table S5). These three MBPs Cg-Def, LCI, and Spinigerin possessed different structures and sizes and their binding performance toward PLA and PS was further evaluated. According to the fluorescence microscopy pictures (Figure 2a) and quantified fluorescence intensity (Figure 2b) of MBPs bound PLA granules, Cg-Def exhibited better PLA binding behavior than LCI and Spinigerin. Moreover, the lower binding strength of Cg-Def to the PS surface than LCI and Spinigerin was observed (Figure 2c). Thus, Cg-Def was selected for further investigation owing to its potential PLA binding specificity compared to PS.

Cg-Def (PDB: 2B68) is an oyster defensin from the mantle of *Crassostrea gigas* with antimicrobial activity against Gram-positive bacteria.[53] Cg-Def with a size of 43 amino acids (4.6 kDa) is composed of an α-helix linked to an antiparallel two-stranded β-sheet by four disulfide bridges.[54] The structure-activity relationship revealed that cysteine residues and aromatic amino acid residues may play key roles in the antimicrobial activity of Cg-Def.[55] So far, the material binding affinity of Cg-Def has not been studied.

2.2. KnowVolution of Cg-Def for Improving PLA Binding Specificity. Prerequisite for a successful directed evolution campaign is a reliable high throughput system, e.g., in 96-well MTP format. Based on a directed evolution campaign to improve the MBP LCI and TA2 for PP- and PS-binding, a suitable screening format,[27,28] which compared binding of Cg-Def from a master plate to two MTP plates (one each composed of PLA and PS), was used (Figure S3). Optimization of high throughput screening assay (i.e., PLA

https://doi.org/10.1021/acscatal.3c02142
ACS Catal. 2023, 13, 12746−12754

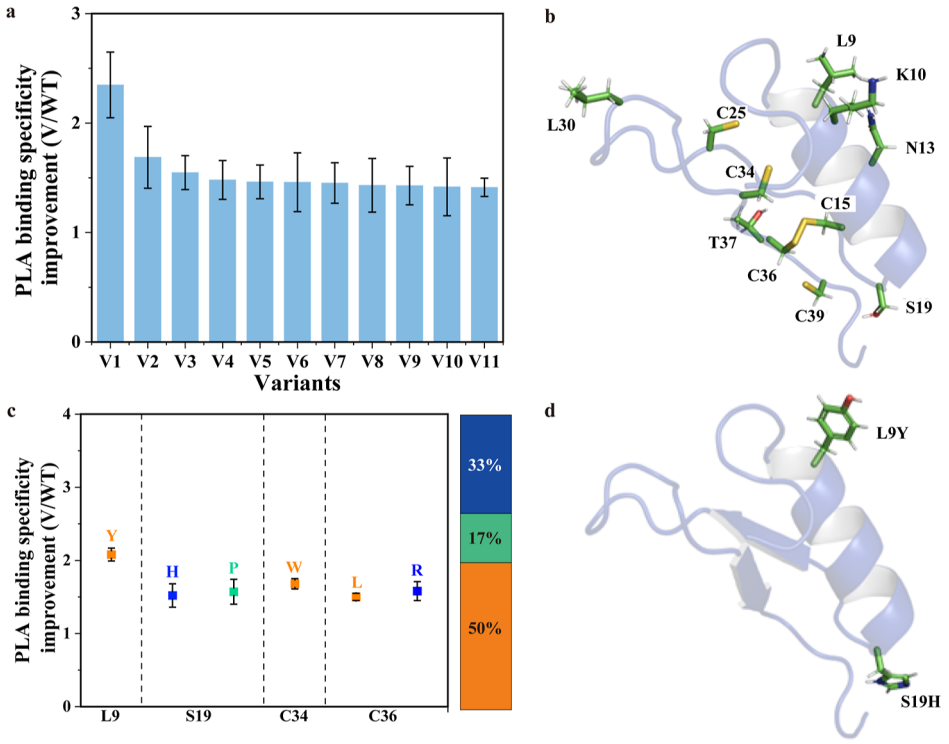

Figure 3. Overview of KnowVolution strategy of Cg-Def for improving PLA binding specificity. (a) Improvement of PLA binding specificity from PS as well as PLA binding strength of 11 variants obtained from Cg-Def epPCR library screening in phase I. The experiments were performed in triplicate. (b) Identified 11 potential key positions of L9, K10, N13, C15, S19, C25, L30, C34, C36, T37, and C39 for PLA binding specificity from PS. (c) Amino acid substitutions in SSM variants with improved PLA binding specificity from PS in phase II. Yellow, blue, and green indicates hydrophobic, positively charged, and neutral amino acids, respectively. The experiment was performed in triplicate. (d) Structure of generated EGFP-Cg-Def YH (L9Y/S19H).

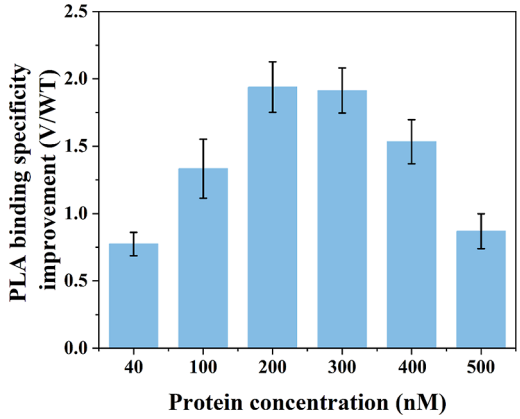

Figure 4. PLA binding specificity improvement with protein concentration of 40−500 nM. The experiments were performed in triplicate.

coating concentration and lysate volume in Figure S4) yielded a coefficient of variation of 18.1 and 13.8% for PLA and PS, respectively (Figure S5), which is generally regarded as a reliable cut off for successfully directed evolution campaigns.[57,58]

Under the optimized conditions of screening assay, the KnowVolution campaign for Cg-Def, which consisted of four phases including identification (phase I), determination (phase II), selection (phase III), and recombination (phase IV), was conducted (Figure S6). In phase I, generation and screening of an epPCR library of Cg-Def were performed to identify the potential key positions for PLA binding specificity. A random mutagenesis library of Cg-Def with 2879 clones was generated with 0.3 mM $MnCl_2$ (mutation frequency: 23 mutations/kb). 20.45% of the library shows improved PLA binding (higher than 1.2 times) than Cg-Def WT. According to the sequences of 11 variants (Table S6) with improved PLA binding specificity (Figure 3a) after library screening, 11 potential key positions (L9, K10, N13, C15, S19, C25, L30, C34, C36, T37, and C39) were identified for PLA binding specificity from PS (Figure 3b).

The identified positions in phase I were subjected for generation of SSM libraries, and beneficial positions were determined after screening the generated SSM libraries. After screening, the variants with 1.5 times improved PLA binding specificity were selected and sequenced (Figure 3c). Notably, positions of L9, S19, C34, and C36 were mainly substituted with hydrophobic or positively charged amino acids, indicating hydrophobic and electrostatic interactions are likely to be the potential mechanism for PLA binding specificity.

In phase III, the computational analysis was performed to select the identified beneficial amino acid substitutions for recombination. Visualization of the 3D structure of Cg-Def showed that, identified positions are mainly located in the α-helix and β-sheet region of Cg-Def. Then CompassR strategy, which provides a selection guide for beneficial substitutions through analysis of the relative free energy of folding ($\Delta\Delta G_{fold}$), was applied for the recombination of these positions (Figure S7).[59] C34W, C36L, and C36R were excluded due to their high $\Delta\Delta G_{fold}$ value. Compared with S19P, the mutation of S19H has lower $\Delta\Delta G_{fold}$ value,

https://doi.org/10.1021/acscatal.3c02142
ACS Catal. 2023, 13, 12746−12754

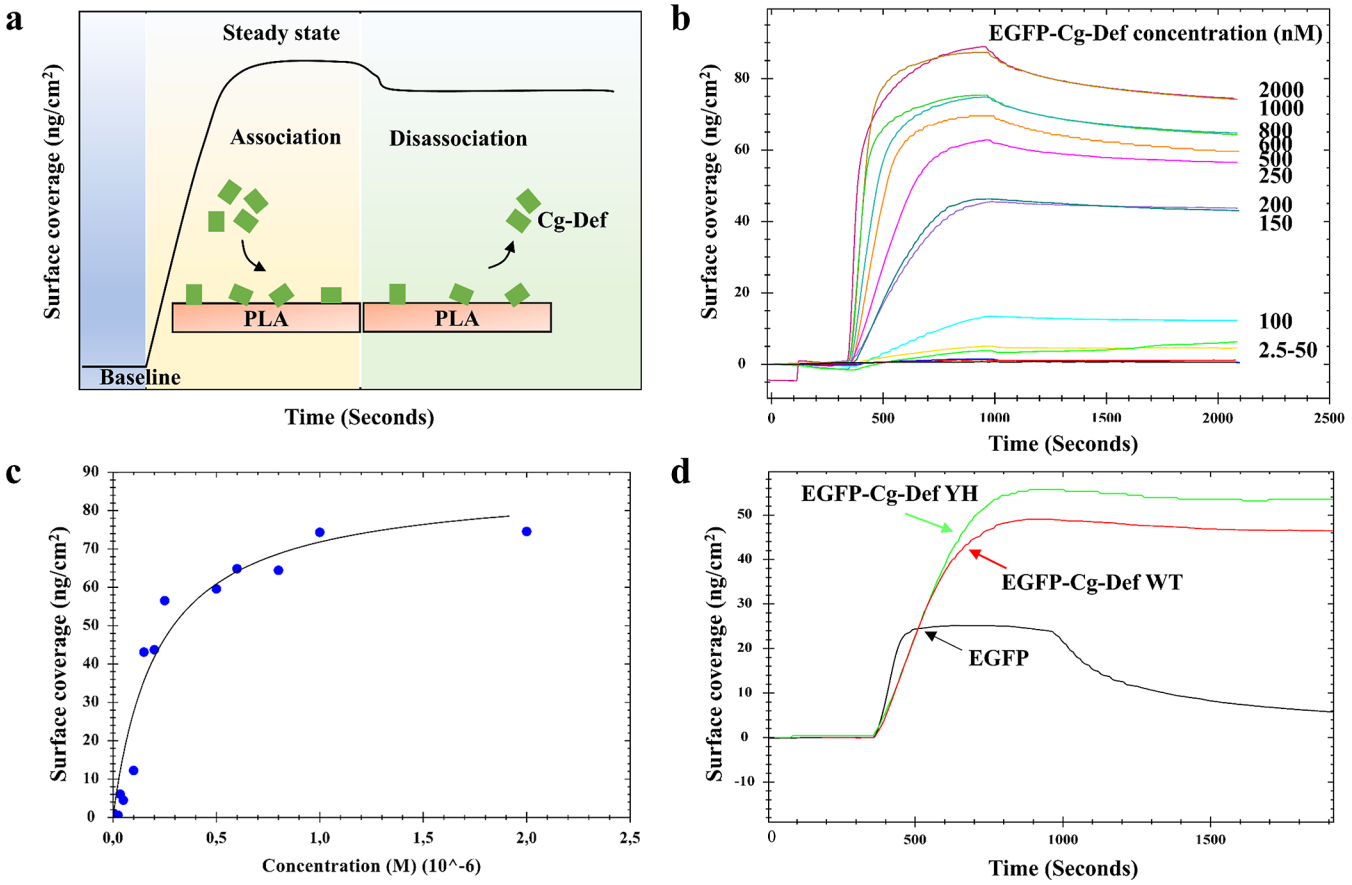

Figure 5. (a) Schematic diagram of Cg-Def adsorption onto PLA chips. (b) Adsorption kinetics of EGFP-Cg-Def on PLA at a range of concentrations between 2.5 and 2000 nM. (c) Langmuir isotherm of EGFP-Cg-Def on PLA at a range of concentrations between 2.5 and 2000 nM. (d) Comparison of surface coverages of EGFP, EGFP-Cg-Def WT, and EGFP-Cg-Def YH at a solution concentration of 500 nM.

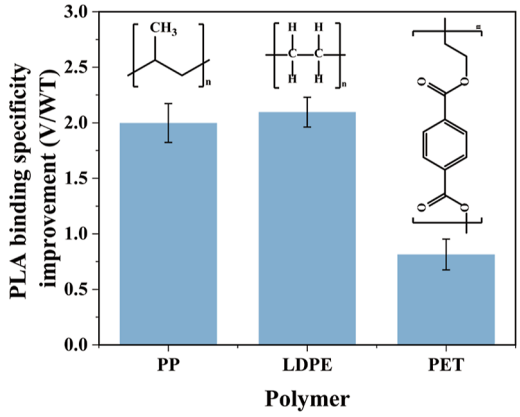

Figure 6. PLA binding specificity improvement from PP, LDPE, and PET (Cg-Def YH VS Cg-Def WT). The concentration of EGFP, EGFP-Cg-Def WT, EGFP-Cg-Def YH was 200 nM. The experiments were performed in triplicate. 1.0-fold improvement of PLA binding specificity indicates that Cg-Def YH exhibits the same PLA binding specificity from PP, LDPE, or PET as Cg-Def WT.

indicating its higher stability.[54] Thus, L9Y and S19H were selected for recombination.

In the end, the recombination of beneficial amino acid substitutions was performed and the PLA binding specificity of recombinants were characterized in phase IV. As L9Y and S19H were identified by CompassR analysis results, one variant EGFP-Cg-Def YH (L9Y/S19H) was generated to investigate its PLA binding specificity from PS (Figure 3d). EGFP, EGFP-Cg-Def WT, and EGFP-Cg-Def YH were expressed and purified for further test (Figure S8).

2.3. PLA Binding Specificity Characterization of Cg-Def Variant. PLA binding specificity of Cg-Def YH was characterized in PLA/PS MTPs with concentration ranging from 40 to 500 nM (Figure 4 and Table S7). The highest PLA binding specificity from PS was 2.0-fold improvement when the protein concentration was 200 or 300 nM. Thus, Cg-Def YH was proved to have enhanced PLA binding specificity from PS.

To quantify the PLA binding specificity more precisely, the PLA binding specificity of Cg-Def YH was measured in the mixed plastic system of PLA/PS films. As shown in Table S8, the ΔPLA/PS ratio of Cg-Def YH was 0.69, which is 1.4-fold higher than WT (0.50), indicating increased amount of Cg-Def YH bind to PLA compared to WT. In addition, the contact angles of PLA and PS films were significantly reduced after coating with Cg-Def WT and Cg-Def YH, indicating increased hydrophilicity of coated PLA and PS films (Figure S9). Additionally, Cg-Def YH-coated PLA film (45.7°) possessed improved hydrophilicity than that of WT (65.1°), which was likely to be caused by the more efficient surface coverage of Cg-Def YH than WT.

Additionally, the adsorption of EGFP-Cg-Def onto PLA was monitored and the binding behavior of WT, Cg-Def YH to PLA were evaluated by SPR (Figure 5). The sensograms consisted of baseline, an association, steady state, and

https://doi.org/10.1021/acscatal.3c02142
ACS Catal. 2023, 13, 12746−12754

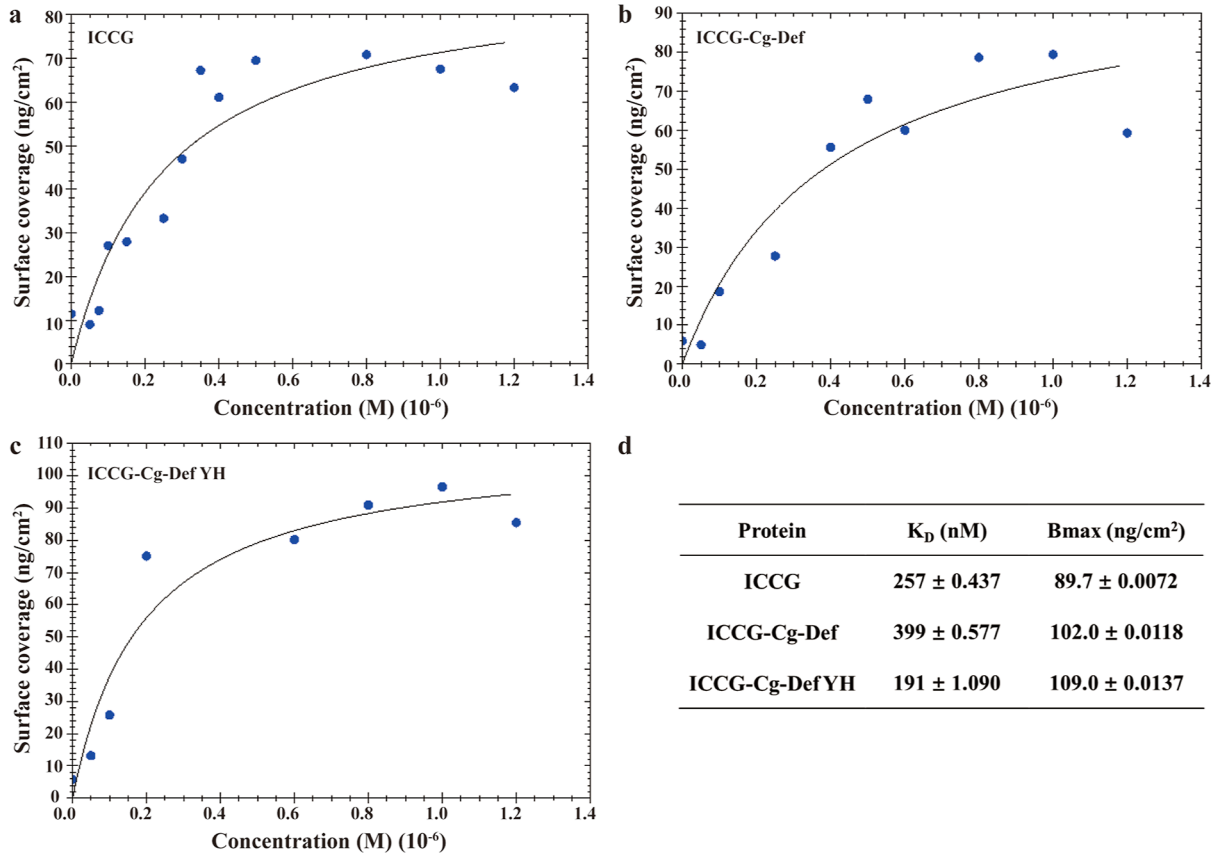

Protein	K_D (nM)	Bmax (ng/cm²)
ICCG	257 ± 0.437	89.7 ± 0.0072
ICCG-Cg-Def	399 ± 0.577	102.0 ± 0.0118
ICCG-Cg-Def YH	191 ± 1.090	109.0 ± 0.0137

Figure 7. PLA binding affinity of ICCG, ICCG-Cg-Def, and ICCG-Cg-Def YH. Langmuir binding isotherms of (a) ICCG, (b) ICCG-Cg-Def, and (c) ICCG-Cg-Def YH on PLA-coated SPR chips. (d) Equilibrium dissociation constant (K_D) values and surface saturation (B_{max}) values of ICCG, ICCG-Cg-Def, and ICCG-Cg-Def YH.

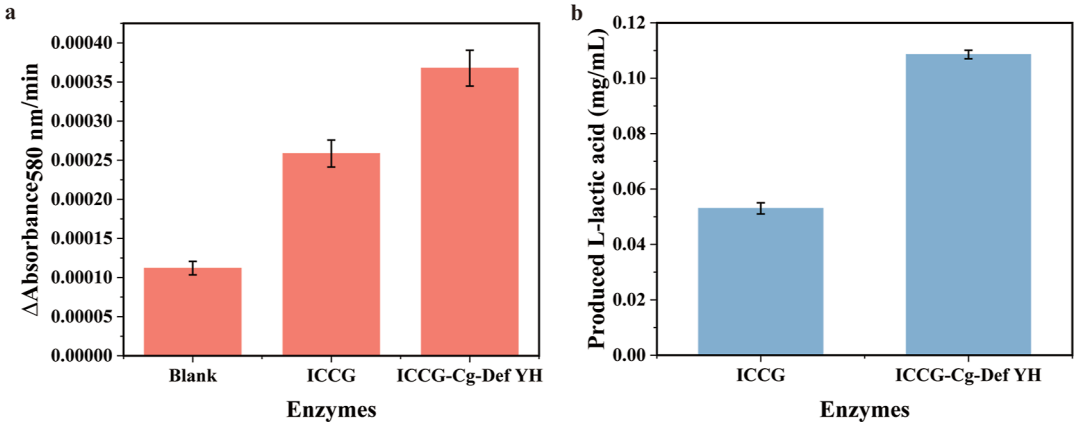

Figure 8. (a) Degradation kinetics of PLA/PS nanoparticle mixture by ICCG WT and ICCG-Cg-Def YH. (b) The L-lactic acid amount produced by ICCG WT and ICCG-Cg-Def YH in degradation of PLA/PS nanoparticle mixture (the L-lactic acid concentration was measured by LDH assay). The PLA/PS mixture (0.105 mg/mL) were degraded by 0.5 μM enzyme at 65 °C for 1 h. The experiments were performed in triplicate.

disassociation phase, which are related to the Tris−HCl running, protein injection, binding equilibrium, and Tris−HCl washing (Figure 5a). The adsorption behavior of EGFP-Cg-Def with a series of concentrations from 2.5 to 2000 nM to PLA chips were recorded in Figure 5b. The equilibrium adsorption of EGFP-Cg-Def was utilized to build adsorption isotherms (Figure 5c). The surface coverage of EGFP-Cg-Def was increased with increasing concentration. The binding of EGFP-Cg-Def became saturated when the EGFP-Cg-Def concentration was 500 nM. The surface coverage reached plateau as the EGFP-Cg-Def concentration was higher than 500 nM. Therefore, the adsorption comparison for EGFP, GFP-Cg-Def WT, and EGFP-Cg-Def YH were conducted at 500 nM (Figure 5d). EGFP-Cg-Def WT and EGFP-Cg-Def YH had significantly higher surface coverage than EGFP. EGFP-Cg-Def YH (53.5 ng/cm^2) displayed improved PLA binding affinity than Cg-Def WT (46.5 ng/cm^2).

To explore the mechanism underlying the high PLA binding specificity of Cg-Def YH from PS, different binding modes of Cg-Def WT and Cg-Def YH on PS and PLA were investigated

https://doi.org/10.1021/acscatal.3c02142
ACS Catal. 2023, 13, 12746−12754

through all-atomistic (aa) molecular dynamics (MD) simulations. These simulations revealed an altered binding mode of Cg-Def YH on PLA that allowed an increase in interaction between Cg-Def YH and PLA compared to Cg-Def WT (Figure S10). On the other hand, the contact frequency between Cg-Def YH and PS is shown to be reduced in comparison to Cg-Def WT. We hypothesize that this increase, respectively the decrease, in interaction between peptide and polymer is responsible for enhanced specificity toward PLA.

Additionally, the PLA binding specificity of Cg-Def YH from other commonly used polymers including PP, low density polyethylene (LDPE), and PET, were measured (Figure 6). Similar to PS, the PLA binding specificity of Cg-Def YH from PP and LDPE also showed 2.0 and 2.1-fold improvement, respectively. However, the improvement of PLA binding specificity from PET was reduced to 0.8 times, which indicated that the engineered Cg-Def YH showed higher binding affinity to PET than Cg-Def WT. The different PLA binding specificity over PET from PS, PP, and PE may be caused by lower hydrophobicity and ester bond of PET. Therefore, our engineered Cg-Def YH could show different binding specificity between hydrophilic and hydrophobic plastics.

2.4. PLA-specific Depolymerization in Mixed Plastics. The binding specificity of engineered Cg-Def variants to PLA in a material-specific manner was validated by PLA-specific depolymerization in a mixed PLA (size: 298 nm, see Figure S11; Mn: 50,000)/PS (size: 525 nm; chain length: 2−400,000 units) nanoparticle suspension. The crystallinities of PLA and PS were measured by X-ray diffraction (XRD). No polymorphic crystalline transition at $2\theta = 16°$ demonstrated that the prepared PLA nanoparticles were amorphous (Figure S12a).[60] The XRD pattern of PS shows a broad peak at approximately 19° that represented its amorphous nature (Figure S12b).[61]

Surprisingly, a very good PLA degrading activity was achieved with an in-house available PET degrading enzyme (leaf-branch compost cutinase ICCG) (Figure S13a). Initially, the effect of temperature on the PLA degradation by ICCG and ICCG-Cg-Def YH was investigated (Figure S13b). The PLA hydrolysis activity of ICCG improved with increasing temperature. In terms of ICCG-Cg-Def YH, the highest hydrolysis activity was observed at 65 °C and it reduced at a higher temperature of 70 °C. ICCG-Cg-Def YH outperformed ICCG at temperature ranging from 50 to 65 °C. To maintain the high PLA degradation efficiency, which benefited from the fused Cg-Def YH, a PLA degradation temperature of 65 °C was determined.

By performing the binding experiments on SPR, Langmuir isotherms of PLA binding at room temperature were generated for ICCG, ICCG-Cg-Def, and ICCG-Cg-Def YH (Figure 7a−c). All of these three proteins bind to PLA. The equilibrium dissociation constant (K_D) values revealed that ICCG-Cg-Def YH displayed best binding affinity to PLA, which is 1.3 times higher than that of ICCG (Figure 7d). The highest PLA surface saturation was achieved by ICCG-Cg-Def YH (109.0 ng/cm^2, 1.2-fold improvement compared to ICCG).

Enhanced PLA-specific depolymerization in mixed PLA/PS was evaluated in pure PLA and PLA/PS mixture. Kinetics of "pure"-PLA degradation of ICCG WT and ICCG-Cg-Def YH (see SDS-PAGE of purified proteins in Figure S14) was determined with PLA nanoparticle suspensions. ICCG-Cg-Def YH has a 1.5-fold faster PLA degradation than ICCG WT (Figure S15). In mixed PLA/PS nanoparticle suspensions (50/50 wt %), ICCG-Cg-Def YH outperformed ICCG WT by 1.4-fold (Figure 8a). The commercial LDH assay kit for L-lactic acid quantification confirmed a two times higher amount of released L-lactic acid for ICCG-Cg-Def YH when compared to ICCG WT (Figure 8b).

Overall, this experiment confirms that PLA depolymerization can be accelerated through enhanced material-specific binding with the MBP Cg-Def. Since ICCG is reported as one of the best-performing PET degrading enzymes, one could expect that a suitable MBP accelerated PET degradation in mixed plastics containing PET. L9 and S19 in Cg-Def were identified as important positions for the PLA-specific binding. In order to further enhance PLA-depolymerization performance, the linker between the MBP and ICCG should be optimized in respect to length and flexibility followed by a directed evolution campaign of the whole ICCG-Cg-Def fusion protein.

3. CONCLUSIONS

In summary, a proof of concept, that material-specific binding accelerated PLA degradation in mixed suspensions of PLA/PS nanoparticles, was achieved through a single KnowVolution campaign (Cg-Def YH with 2-fold improved PLA degradation). We are convinced that the presented approach (enhanced material-specific binding and fusion of MBP to polymer degrading enzymes) can generally be applied in a material-specific degradation and recycling of many mixed-plastics (e.g., the employed ICCG degrades PET too). We see a high potential that the proposed approach enables and contributes to a circular economy of plastics, so that plastics can be used in a sustainable way by future generations.

■ ASSOCIATED CONTENT

Supporting Information

The Supporting Information is available free of charge at https://pubs.acs.org/doi/10.1021/acscatal.3c02142.

Materials and methods; sequences of MBPs and ICCG fusion constructs; selection, expression, characterization, and computational analysis of Cg-Def YH for PLA binding specificity; XRD of PLA and PS nanoparticles; and selection and degradation temperature optimization of PLA degradation enzyme (PDF)

■ AUTHOR INFORMATION

Corresponding Authors

Yu Ji − *Institute of Biotechnology, RWTH Aachen University, Aachen 52074, Germany*; Email: yu.ji@biotec.rwth-aachen.de

Ulrich Schwaneberg − *Institute of Biotechnology, RWTH Aachen University, Aachen 52074, Germany; DWI-Leibniz Institute for Interactive Materials, Aachen 52074, Germany*; orcid.org/0000-0003-4026-701X; Email: u.schwaneberg@biotec.rwth-aachen.de

Authors

Yi Lu − *Institute of Biotechnology, RWTH Aachen University, Aachen 52074, Germany*

Kai-Wolfgang Hintzen − *Institute of Biotechnology, RWTH Aachen University, Aachen 52074, Germany; DWI-Leibniz Institute for Interactive Materials, Aachen 52074, Germany*

Tetiana Kurkina − *Institute of Biotechnology, RWTH Aachen University, Aachen 52074, Germany*

https://doi.org/10.1021/acscatal.3c02142
ACS Catal. 2023, 13, 12746−12754

Complete contact information is available at:
https://pubs.acs.org/10.1021/acscatal.3c02142

Author Contributions

U.S. designed the concept. Y.L., Y.J., and U.S. conceived of and designed the experiments; Y.L. performed the experiments and analyzed the data; Y.L. wrote the manuscript; K.-W.H. did the computational analysis; Y.J., T.K., and U.S. revised the manuscript. All authors have given approval to the final version of the manuscript.

Notes

The authors declare no competing financial interest.

■ ACKNOWLEDGMENTS

This work was supported by the China Scholarship Council (CSC) and the European Union's Horizon 2020 research and innovation program under grant agreement no. 870294 for the project MIX-UP. The authors thank Shuaiqi Meng for CompassR analysis and Dr. Tamás Haraszti for XRD measurement.

■ REFERENCES

(1) Sardon, H.; Dove, A. P. Plastics recycling with a difference. *Science* **2018**, *360*, 380−381.
(2) *Plastics-the Facts 2022*; 2022.
(3) Provencher, J.; Liboiron, M.; Borrelle, S.; Bond, A.; Rochman, C.; Lavers, J.; Avery-Gomm, S.; Yamashita, R.; Ryan, P.; Lusher, A.; Hammer, S.; Bradshaw, H.; Khan, J.; Mallory, M. A Horizon Scan of research priorities to inform policies aimed at reducing the harm of plastic pollution to biota. *Sci. Total Environ.* **2020**, *733*, 139381.
(4) Ji, J. H.; Zhao, T.; Li, F. H. Remediation technology towards zero plastic pollution: recent advance and perspectives. *Environ. Pollut.* **2022**, *313*, 120166.
(5) Yuan, Z. H.; Nag, R.; Cummins, E. Human health concerns regarding microplastics in the aquatic environment- From marine to food systems. *Sci. Total Environ.* **2022**, *823*, 153730.
(6) Shen, M. C.; Song, B.; Zeng, G. M.; Zhang, Y. X.; Huang, W.; Wen, X. F.; Tang, W. W. Are biodegradable plastics a promising solution to solve the global plastic pollution? *Environ. Pollut.* **2020**, *263*, 114469.
(7) Law, K. L.; Narayan, R. Reducing environmental plastic pollution by designing polymer materials for managed end-of-life. *Nat. Rev. Mater.* **2021**, *7*, 104−116.
(8) Xia, C.; Lam, S. S.; Zhong, H.; Fabbri, E.; Sonne, C. Assess and reduce toxic chemicals in bioplastics. *Science* **2022**, *378*, 842.
(9) Xia, Q. Q.; Chen, C. J.; Yao, Y. G.; Li, J. G.; He, S. M.; Zhou, Y. B.; Li, T.; Pan, X. J.; Yao, Y.; Hu, L. B. A strong, biodegradable and recyclable lignocellulosic bioplastic. *Nat. Sustain.* **2021**, *4*, 627−635.
(10) Mahmoodi, A.; Ghodrati, S.; Khorasani, M. High-strength, low-permeable, and light-protective nanocomposite films based on a hybrid nanopigment and biodegradable PLA for food packaging applications. *ACS Omega* **2019**, *4*, 14947−14954.
(11) Su, S.; Kopitzky, R.; Tolga, S.; Kabasci, S. Polylactide (PLA) and its blends with poly(butylene succinate) (PBS): a brief review. *Polymers* **2019**, *11*, 1193.
(12) Lekube, B. M.; Burgstaller, C. Study of mechanical and rheological properties, morphology, and miscibility in polylactid acid blends with thermoplastic polymers. *J. Appl. Polym. Sci.* **2022**, *139*, 51662.
(13) Hamad, K.; Kaseem, M.; Ayyoob, M.; Joo, J.; Deri, F. Polylactic acid blends: the future of green, light and tough. *Prog. Polym. Sci.* **2018**, *85*, 83−127.
(14) Min, K.; Cuiffi, J. D.; Mathers, R. T. Ranking environmental degradation trends of plastic marine debris based on physical properties and molecular structure. *Nat. Commun.* **2020**, *11*, 727.
(15) Meides, N.; Menzel, T.; Poetzschner, B.; Loder, M. G. J.; Mansfeld, U.; Strohriegl, P.; Altstaedt, V.; Senker, J. Reconstructing the environmental degradation of polystyrene by accelerated weathering. *Environ. Sci. Technol.* **2021**, *55*, 7930−7938.
(16) Liu, S.; Qin, S. H.; He, M.; Zhou, D. F.; Qin, Q. D.; Wang, H. Current applications of poly(lactic acid) composites in tissue engineering and drug delivery. *Composites, Part B* **2020**, *199*, 108238.
(17) Gebrekrstos, A.; Ray, S. S. Superior electrical conductivity and mechanical properties of phase-separated polymer blend composites by tuning the localization of nanoparticles for electromagnetic interference shielding applications. *J. Polym. Sci.* **2023**, 1−18.
(18) Zuo, X. H.; Xue, Y.; Wang, L. K.; Zhou, Y. C.; Yin, Y. F.; Chuang, Y. C.; Chang, C. C.; Yin, R. L.; Rafailovich, M. H.; Guo, Y. C. Engineering styrenic blends with poly(lactic acid). *Macromolecules* **2019**, *52*, 7547−7556.
(19) Li, Y.; Pionteck, J.; Pötschke, P.; Voit, B. Thermal annealing to influence the vapor sensing behavior of co-continuous poly(lactic acid)/polystyrene/multiwalled carbon nanotube composites. *Mater. Des.* **2020**, *187*, 108383.
(20) Shao, L.; Chang, Y. C.; Hao, C.; Fei, M. E.; Zhao, B. M.; Bliss, B. J.; Zhang, J. W. A chemical approach for the future of PLA upcycling: from plastic wastes to new 3D printing materials. *Green Chem.* **2022**, *24*, 8716−8724.
(21) Bagheri, A. R.; Laforsch, C.; Greiner, A.; Agarwal, S. Fate of so-called biodegradable polymers in seawater and freshwater. *Global chall.* **2017**, *1*, 1700048.
(22) Rosenboom, J. G.; Langer, R.; Traverso, G. Bioplastics for a circular economy. *Nat. Rev. Mater.* **2022**, *7*, 117−137.
(23) Sullivan, K. P.; Werner, A. Z.; Ramirez, K. J.; Ellis, L. D.; Bussard, J. R.; Black, B. A.; Brandner, D. G.; Bratti, F.; Buss, B. L.; Dong, X.; Haugen, S. J.; Ingraham, M. A.; Konev, M. O.; Michener, W. E.; Miscall, J.; Pardo, I.; Woodworth, S. P.; Guss, A. M.; Roman-Leshkov, Y.; Stahl, S. S.; Beckham, G. T. Mixed plastics waste valorization through tandem chemical oxidation and biological funneling. *Science* **2022**, *378*, 207−211.
(24) Tournier, V.; Duquesne, S.; Guillamot, F.; Cramail, H.; Taton, D.; Marty, A.; André, I. Enzymes? Power for Plastics Degradation. *Chem. Rev.* **2023**, *123*, 5612−5701.
(25) Kawai, F.; Nakadai, K.; Nishioka, E.; Nakajima, H.; Ohara, H.; Masaki, K.; Iefuji, H. Different enantioselectivity of two types of poly(lactic acid) depolymerases toward poly(L-lactic acid) and poly(D-lactic acid). *Polym. Degrad. Stab.* **2011**, *96*, 1342−1348.
(26) Ribitsch, D.; Hromic, A.; Zitzenbacher, S.; Zartl, B.; Gamerith, C.; Pellis, A.; Jungbauer, A.; Lyskowski, A.; Steinkellner, G.; Gruber, K.; Tscheliessnig, R.; Herrero Acero, E.; Guebitz, G. M. Small cause, large effect: structural characterization of cutinases from *Thermobifida cellulosilytica*. *Biotechnol. Bioeng.* **2017**, *114*, 2481−2488.
(27) Rubsam, K.; Davari, M. D.; Jakob, F.; Schwaneberg, U. KnowVolution of the polymer-binding peptide LCI for improved polypropylene binding. *Polymers* **2018**, *10*, 423.
(28) Rubsam, K.; Weber, L.; Jakob, F.; Schwaneberg, U. Directed evolution of polypropylene and polystyrene binding peptides. *Biotechnol. Bioeng.* **2018**, *115*, 321−330.
(29) Zou, Z.; Mate, D. M.; Rubsam, K.; Jakob, F.; Schwaneberg, U. Sortase-mediated high-throughput screening platform for directed enzyme evolution. *ACS Comb. Sci.* **2018**, *20*, 203−211.
(30) Apitius, L.; Buschmann, S.; Bergs, C.; Schonauer, D.; Jakob, F.; Pich, A.; Schwaneberg, U. Biadhesive peptides for assembling stainless steel and compound loaded micro-containers. *Macromol. Biosci.* **2019**, *19*, 1900125.
(31) Dedisch, S.; Wiens, A.; Davari, M. D.; Soder, D.; Rodriguez-Emmenegger, C.; Jakob, F.; Schwaneberg, U. Matter-tag: A universal immobilization platform for enzymes on polymers, metals, and silicon-based materials. *Biotechnol. Bioeng.* **2020**, *117*, 49−61.
(32) Meurer, R. A.; Kemper, S.; Knopp, S.; Eichert, T.; Jakob, F.; Goldbach, H. E.; Schwaneberg, U.; Pich, A. Biofunctional microgel-based fertilizers for controlled foliar delivery of nutrients to plants. *Angew. Chem., Int. Ed.* **2017**, *56*, 7380−7386.

(33) Kuhn, T.; Möhring, N.; Töpel, A.; Jakob, F.; Britz, W.; Broring, S.; Pich, A.; Schwaneberg, U.; Rennings, M. Using a bio-economic farm model to evaluate the economic potential and pesticide load reduction of the greenRelease technology. *Agric. Syst.* **2022**, *201*, 103454.
(34) Schwinges, P.; Pariyar, S.; Jakob, F.; Rahimi, M.; Apitius, L.; Hunsche, M.; Schmitt, L.; Noga, G.; Langenbach, C.; Schwaneberg, U.; Conrath, U. A bifunctional dermaseptin-thanatin dipeptide functionalizes the crop surface for sustainable pest management. *Green Chem.* **2019**, *21*, 2316−2325.
(35) Rubsam, K.; Stomps, B.; Boker, A.; Jakob, F.; Schwaneberg, U. Anchor peptides: a green and versatile method for polypropylene functionalization. *Polymer* **2017**, *116*, 124−132.
(36) Cheng, F.; Zhu, L. L.; Schwaneberg, U. Directed evolution 2.0: improving and deciphering enzyme properties. *Chem. Commun.* **2015**, *51*, 9760−9772.
(37) Islam, S.; Laaf, D.; Infanzon, B.; Pelantova, H.; Davari, M. D.; Jakob, F.; Kren, V.; Elling, L.; Schwaneberg, U. KnowVolution campaign of an aryl sulfotransferase increases activity toward cellobiose. *Chem. Eur J.* **2018**, *24*, 17117−17124.
(38) Contreras, F.; Thiele, M. J.; Pramanik, S.; Rozhkova, A. M.; Dotsenko, A. S.; Zorov, I. N.; Sinitsyn, A. P.; Davari, M. D.; Schwaneberg, U. KnowVolution of a GH5 cellulase from *Penicillium verruculosum* to improve thermal stability for biomass degradation. *ACS Sustain. Chem. Eng.* **2020**, *8*, 12388−12399.
(39) Novoa, C.; Dhoke, G. V.; Mate, D. M.; Martinez, R.; Haarmann, T.; Schreiter, M.; Eidner, J.; Schwerdtfeger, R.; Lorenz, P.; Davari, M. D.; Jakob, F.; Schwaneberg, U. KnowVolution of a fungal laccase toward alkaline pH. *ChemBioChem* **2019**, *20*, 1458−1466.
(40) Ji, Y.; Islam, S.; Cui, H. Y.; Dhoke, G. V.; Davari, M. D.; Mertens, A. M.; Schwaneberg, U. Loop engineering of aryl sulfotransferase B for improving catalytic performance in regioselective sulfation. *Catal. Sci. Technol.* **2020**, *10*, 2369−2377.
(41) Wallraf, A. M.; Liu, H. F.; Zhu, L. L.; Khalfallah, G.; Simons, C.; Alibiglou, H.; Davari, M. D.; Schwaneberg, U. A loop engineering strategy improves laccase lcc2 activity in ionic liquid and aqueous solution. *Green Chem.* **2018**, *20*, 2801−2812.
(42) Mandawe, J.; Infanzon, B.; Eisele, A.; Zaun, H.; Kuballa, J.; Davari, M. D.; Jakob, F.; Elling, L.; Schwaneberg, U. Directed evolution of hyaluronic acid synthase from *Pasteurella multocida* towards high-molecular-weight hyaluronic acid. *ChemBioChem* **2018**, *19*, 1414−1423.
(43) Cicortas Gunnarsson, L.; Montanier, C.; Tunnicliffe, R. B.; Williamson, M. R.; Gilbert, H. J.; Nordberg Karlsson, E.; Ohlin, M. Novel xylan-binding properties of an engineered family 4 carbohydrate-binding module. *Biochem. J.* **2007**, *406*, 209−214.
(44) Nakamura, A.; Tsukada, T.; Auer, S.; Furuta, T.; Wada, M.; Koivula, A.; Igarashi, K.; Samejima, M. The tryptophan residue at the active site tunnel entrance of *Trichoderma reesei* cellobiohydrolase Cel7A is important for initiation of degradation of crystalline cellulose. *J. Biol. Chem.* **2013**, *288*, 13503−13510.
(45) Wei, R.; von Haugwitz, G.; Pfaff, L.; Mican, J.; Badenhorst, C. P. S.; Liu, W. D.; Weber, G.; Austin, H. P.; Bednar, D.; Damborsky, J.; Bornscheuer, U. T. Mechanism-based design of efficient PET hydrolases. *ACS Catal.* **2022**, *12*, 3382−3396.
(46) Graham, R.; Erickson, E.; Brizendine, R. K.; Salvachua, D.; Michener, W. E.; Li, Y. H.; Tan, Z. P.; Beckham, G. T.; McGeehan, J. E.; Pickford, A. R. The role of binding modules in enzymatic poly(ethylene terephthalate) hydrolysis at high-solids loadings. *Chem Catal.* **2022**, *2*, 2644−2657.
(47) Hwang, D. H.; Lee, M. E.; Cho, B. H.; Oh, J. W.; You, S. K.; Ko, Y. J.; Hyeon, J. E.; Han, S. O. Enhanced biodegradation of waste poly(ethylene terephthalate) using a reinforced plastic degrading enzyme complex. *Sci. Total Environ.* **2022**, *842*, 156890.
(48) Xue, R.; Chen, Y.; Rong, H.; Wei, R.; Cui, Z.; Zhou, J.; Dong, W.; Jiang, M. Fusion of chitin-binding domain from *Chitinolyticbacter meiyuanensis* SYBC-H1 to the leaf-branch compost cutinase for enhanced PET hydrolysis. *Front. Bioeng. Biotechnol.* **2021**, *9*, 762854.
(49) Islam, S.; Apitius, L.; Jakob, F.; Schwaneberg, U. Targeting microplastic particles in the void of diluted suspensions. *Environ. Int.* **2019**, *123*, 428−435.
(50) Rennison, A. P.; Westh, P.; Moller, M. S. Protein-plastic interactions: The driving forces behind the high affinity of a carbohydrate-binding module for polyethylene terephthalate. *Sci. Total Environ.* **2023**, *870*, 161948.
(51) Chen, Z. Z.; Duan, R. D.; Xiao, Y. J.; Wei, Y.; Zhang, H. X.; Sun, X. Z.; Wang, S.; Cheng, Y. Y.; Wang, X.; Tong, S. W.; Yao, Y. X.; Zhu, C.; Yang, H. T.; Wang, Y. Y.; Wang, Z. F. Biodegradation of highly crystallized poly(ethylene terephthalate) through cell surface codisplay of bacterial PETase and hydrophobin. *Nat. Commun.* **2022**, *13*, 7138.
(52) Tournier, V.; Topham, C. M.; Gilles, A.; David, B.; Folgoas, C.; Moya-Leclair, E.; Kamionka, E.; Desrousseaux, M. L.; Texier, H.; Gavalda, S.; Cot, M.; Guemard, E.; Dalibey, M.; Nomme, J.; Cioci, G.; Barbe, S.; Chateau, M.; Andre, I.; Duquesne, S.; Marty, A. An engineered PET depolymerase to break down and recycle plastic bottles. *Nature* **2020**, *580*, 216−219.
(53) Schmitt, P.; Rosa, R. D.; Destoumieux-Garzon, D. An intimate link between antimicrobial peptide sequence diversity and binding to essential components of bacterial membranes. *Biochim. Biophys. Acta Biomembr.* **2016**, *1858*, 958−970.
(54) Gueguen, Y.; Herpin, A.; Aumelas, A.; Garnier, J.; Fievet, J.; Escoubas, J. M.; Bulet, P.; Gonzalez, M.; Lelong, C.; Favrel, P.; Bachere, E. Characterization of a defensin from the oyster *Crassostrea gigas* - recombinant production, folding, solution structure, antimicrobial activities, and gene expression. *J. Biol. Chem.* **2006**, *281*, 313−323.
(55) Hao, L. L.; Wang, X. C.; Cao, Y. R.; Xu, J.; Xue, C. H. A comprehensive review of oyster peptides: preparation, characterisation and bioactivities. *Rev. Aquacult.* **2022**, *14*, 120−138.
(56) Schneider, C. A.; Rasband, W. S.; Eliceiri, K. W. NIH Image to ImageJ: 25 years of image analysis. *Nat. Methods* **2012**, *9*, 671−675.
(57) Zhu, L. L.; Tee, K. L.; Roccatano, D.; Sonmez, B.; Ni, Y.; Sun, Z. H.; Schwaneberg, U. Directed evolution of an antitumor drug (arginine deiminase PpADI) for increased activity at physiological pH. *ChemBioChem* **2010**, *11*, 691−697.
(58) Brands, S.; Brass, H. U. C.; Klein, A. S.; Pietruszka, J.; Ruff, A. J.; Schwaneberg, U. A colourimetric high-throughput screening system for directed evolution of prodigiosin ligase PigC. *Chem. Commun.* **2020**, *56*, 8631−8634.
(59) Cui, H. Y.; Cao, H.; Cai, H. Y.; Jaeger, K. E.; Davari, M. D.; Schwaneberg, U. Computer-Assisted Recombination (CompassR) teaches us how to recombine beneficial substitutions from directed evolution campaigns. *Chem. Eur J.* **2020**, *26*, 643−649.
(60) Chu, Z.; Zhao, T.; Li, L.; Fan, J.; Qin, Y. Characterization of antimicrobial poly (lactic acid)/nano-composite films with silver and zinc oxide nanoparticles. *Materials* **2017**, *10*, 659.
(61) Chaudhary, A. K.; Vijayakumar, R. P. Synthesis of polystyrene/starch/CNT composite and study on its biodegradability. *J. Polym. Res.* **2020**, *27*, 187.

https://doi.org/10.1021/acscatal.3c02142
ACS Catal. 2023, 13, 12746−12754